

# Clathrin-mediated Endocytosis of MUC1 Is Modulated by Its Glycosylation State

Yoram Altschuler,\* Carol L. Kinlough,<sup>†</sup> Paul A. Poland,<sup>†</sup> James B. Bruns,<sup>†</sup> Gerard Apodaca,<sup>†</sup> Ora A. Weisz,<sup>†</sup> and Rebecca P. Hughey<sup>†‡</sup>

\*Department of Anatomy, University of California San Francisco, San Francisco, California 94143; and

<sup>†</sup>Laboratory of Epithelial Cell Biology, Department of Medicine, Renal-Electrolyte Division, University of Pittsburgh, Pittsburgh, Pennsylvania 15261

Submitted November 8, 1999; Accepted December 21, 1999

Monitoring Editor: Susanne Pfeffer

MUC1 is a mucin-like type 1 transmembrane protein associated with the apical surface of epithelial cells. In human tumors of epithelial origin MUC1 is overexpressed in an underglycosylated form with truncated *O*-glycans and accumulates in intracellular compartments. To understand the basis for this altered subcellular localization, we compared the synthesis and trafficking of various glycosylated forms of MUC1 in normal (Chinese hamster ovary) cells and glycosylation-defective (ldID) cells that lack the epimerase to make UDP-Gal/GalNAc from UDP-Glc/GlcNAc. Although the MUC1 synthesized in ldID cells was rapidly degraded, addition of GalNAc alone to the culture media resulted in stabilization and near normal surface expression of MUC1 with truncated but sialylated *O*-glycans. Interestingly, the initial rate of endocytosis of this underglycosylated MUC1 was stimulated by twofold compared with fully glycosylated MUC1. However, the half-lives of the two forms were not different, indicating that trafficking to lysosomes was not affected. Both the normal and stimulated internalization of MUC1 could be blocked by hypertonic media, a hallmark of clathrin-mediated endocytosis. MUC1 endocytosis was also blocked by expression of a dominant-negative mutant of dynamin-1 (K44A), and MUC1 was observed in both clathrin-coated pits and vesicles by immunoelectron microscopy of ultrathin cryosections. Our data suggest that the subcellular redistribution of MUC1 in tumor cells could be a direct result of altered endocytic trafficking induced by its aberrant glycosylation; potential models are discussed. These results also implicate a new role for *O*-glycans on mucin-like membrane proteins entering the endocytic pathway through clathrin-coated pits.

## INTRODUCTION

Oligosaccharides on proteins have a multifunctional role in the folding, stability, and targeting of glycoproteins. *N*-glycans, which are added during translocation of proteins in the endoplasmic reticulum, are used by the chaperones calnexin and calreticulin to retain glycoproteins within this compartment until they are properly folded (Trowbridge and Helenius, 1998). In the case of soluble lysosomal proteins, the *N*-glycans are altered for recognition and proper delivery of the proteins by the mannose-6-phosphate receptor (Kornfeld, 1987), whereas *N*-glycans on some soluble proteins are

required for their polarized delivery to the apical surface of epithelial cells (Scheiffele *et al.*, 1995). The role of *O*-glycans on glycoproteins is less well understood, although it is clear that both *N*- and *O*-glycans on proteins can provide protection from degradation. In one case, clusters of *O*-glycans can act as an apical targeting signal for either the transmembrane or soluble form of the neurotrophin receptor (Yeaman *et al.*, 1997). Furthermore, specific *O*-glycans on endothelial mucins can act as intercellular ligands for molecules such as selectins (Rosen and Bertozzi, 1994). However, the role that oligosaccharides play in the regulation of glycoprotein trafficking in the endocytic pathway is undefined.

Human MUC1 is a type I transmembrane protein with a mucin-like ectodomain resulting from extensive glycosylation of a variable number of tandem repeats (40–90 copies) (Gendler *et al.*, 1991; Hilkens *et al.*, 1992). These perfect repeats of 20 residues (PDTRPAPGSTAPPAHGVTS) have five threonines and serines that are all modified with mucin-type *O*-linked glycans (Hanisch *et al.*, 1989; Hull *et al.*, 1989; Lloyd *et al.*, 1996), and this domain is flanked by imperfect

<sup>‡</sup> Corresponding author. E-mail address: hughey@msx.dept-med.pitt.edu.

Abbreviations used: Cys, cysteine; DOX, doxycycline; Gal (G), galactose; GalNAc (GN), *N*-acetylgalactosamine; hCAR, human coxsackievirus and adenovirus receptor; HBS, HEPES-buffered saline; MESNA, 2-mercaptoethanesulfonic acid; Met, methionine; pIgR, polymeric immunoglobulin receptor.

repeats with fewer glycosylation sites. In addition to O-linked glycosylation, MUC1 contains five consensus sites for N-linked glycan addition in a nonrepetitive sequence adjacent to the single transmembrane domain. The 72-residue carboxy-terminal cytoplasmic domain contains seven tyrosine residues, at least one of which can be phosphorylated (Zrihan-Licht *et al.*, 1994; Pandey *et al.*, 1995); phosphorylation of the tyrosine furthest from the membrane promotes interaction with the SH2 domain of the adaptor protein Grb2 (Pandey *et al.*, 1995), which can bind proteins such as the Sos exchange protein of Ras (Chardin *et al.*, 1993; Egan *et al.*, 1993) or the PRD domain of the GTPase dynamin (Barylko *et al.*, 1998). Thus, MUC1 is a complex molecule that is likely to function as more than a simple membrane-anchored mucin.

Litvinov and Hilken (1993) have shown that an immature, incompletely sialylated form of MUC1 appears at the cell surface in mammary epithelial cells and matures by addition of more sialic acid during several rounds of recycling, and recycling continues even after full maturation. However, there is a significant increase in intracellular staining for MUC1 in breast (Ceriani *et al.*, 1992) and thyroid (Bièche *et al.*, 1997) carcinomas when compared with normal epithelia, and the prevalence of intracellular MUC1 in breast cancer correlates with a poor prognosis for the patient (Ceriani *et al.*, 1992). The basis for this intracellular accumulation is not known but could result from altered kinetics of membrane trafficking either in the *de novo* pathway or in the endosomal, recycling pathway. Because MUC1 is found in an underglycosylated state in many tumors, we have compared the trafficking and maturation of MUC1 in normal Chinese hamster ovary (CHO) cells and glycosylation-defective CHO cells (ldID cells) that lack the epimerase to make UDP-Gal and -GalNAc from UDP-Glc and -GlcNAc, respectively (Kingsley *et al.*, 1986). This defect completely blocks O-linked glycosylation of proteins and prevents maturation of N-linked glycans. Addition of Gal and GalNAc to the media of ldID cells can reverse this phenotype, and addition of GalNAc alone results in synthesis of proteins with truncated O-linked glycans, a structure observed on MUC1 in many tumor cells (Hull *et al.*, 1989; Lloyd *et al.*, 1996). Using MUC1 expression in both CHO and ldID cells, we are now able to evaluate the effect of MUC1 underglycosylation on its subsequent internalization. In fact, our present studies on the trafficking of the mucin-like MUC1 indicate that alterations in O-glycan structure can stimulate its endocytosis and intracellular accumulation without enhancing the degradation of the molecule.

## MATERIALS AND METHODS

### Cell Culture

Clonal cultures of normal CHO and glycosylation-defective CHO cells (ldID cells) expressing human MUC1 with 22 tandem repeats were obtained by transfection of cells with recombinant MUC1 cDNA in the pREP4 plasmid (Invitrogen, San Diego, CA), followed by clonal selection and maintenance in media containing hygromycin (0.4 mg/ml) as described previously (Poland *et al.*, 1997). Clonal cell lines expressing the human coxsackie adenovirus receptor protein (hCAR; Bergelson *et al.*, 1997) were obtained by transfection of MUC1-expressing CHO or ldID cells with the hCAR cDNA in the pcDNA3.1 vector (Invitrogen), followed by clonal selection in media containing G418 (0.5 mg/ml); the resulting cell lines were subsequently maintained in both G418 and hygromycin. A cell line ex-

pressing the polymeric immunoglobulin receptor (pIgR) was prepared by transfection of ldID cells with the rabbit pIgR cDNA subcloned into the pCB7 vector (Mostov *et al.*, 1986); clonal lines were selected in media containing hygromycin. All cell lines were maintained in Dulbecco's minimum Eagle's medium (DMEM) and Ham's F12 (1:1) with 3% fetal bovine serum (normal culture media) at 37°C in 5% CO<sub>2</sub>. All tissue culture reagents were purchased from Life Technologies (Gaithersburg, MD).

### Radiolabeling, Biotinylation, and Immunoprecipitation of MUC1

Confluent cultures of cells in 35-mm dishes were washed once with 1 ml of DME media lacking methionine and cysteine (Met/Cys; ICN, Costa Mesa, CA) and starved for Met and Cys in 1 ml of the same media for 15 min before addition of 50–100  $\mu$ Ci of [<sup>35</sup>S]Met/Cys (Easy Tag Express-[<sup>35</sup>S]Protein Labeling Mixture; New England Nuclear, Wilmington, DE) for the indicated time. Labeled cells were chased in normal culture medium. Where specified, media used to starve, pulse, and chase cells was supplemented with either Gal or GalNAc at the levels indicated in each experiment. After the chase period, cells were rapidly chilled on ice for biotinylation of cell surface proteins as previously described (Gottardi and Caplan, 1992). Briefly, cells were washed four times with 1 ml of phosphate buffered saline (PBS; 137 mM NaCl, 2.6 mM KCl, 15.2 mM Na<sub>2</sub>HPO<sub>4</sub>, 1.47 mM KH<sub>2</sub>PO<sub>4</sub>, 0.5 mM MgCl<sub>2</sub>, and 0.7 mM CaCl<sub>2</sub>) and incubated with 0.5 mg/ml sulfosuccinimidyl-2-(biotinamido)-ethyl-1,3-dithiopropionate-biotin (Pierce, Rockford, IL) in TEA-buffered saline (10 mM triethanolamine, pH 7.6, 137 mM NaCl, and 1 mM CaCl<sub>2</sub>) for 10 min. The reaction was quenched by washing the cells three times with normal culture media. Cells were solubilized at room temperature with 0.2 ml of 60 mM *n*-octyl  $\beta$ -D-glucopyranoside and 0.1% SDS (both from Sigma, St. Louis, MO) in HEPES-buffered saline (HBS, 10 mM HEPES-NaOH, pH 7.4, 150 mM NaCl) for 20 min, and insoluble material was removed by centrifugation in a microcentrifuge at 14,000 rpm for 7 min. Supernatants were recovered and rotated end-over-end overnight at 4°C after addition of protein G immobilized on Sepharose 4B (Sigma) and mouse monoclonal antibodies VU-3-C6 against the tandem repeat domain (Rye *et al.*, 1998) and 232A1 against an extracellular nontandem repeat domain (Oosterkamp *et al.*, 1997). Immunoprecipitates were recovered by brief centrifugation and washed once with 0.5 ml each: 1% Triton X-100 (Boehringer Mannheim, Indianapolis, IN) in HBS, 0.01% SDS in HBS, and finally HBS. Where indicated, the pellets were resuspended in acetate buffer (50 mM sodium acetate, pH 5.5, 0.15 M NaCl, 9 mM CaCl<sub>2</sub>) and incubated with or without 1 mU neuraminidase (*Vibrio cholera*; Calbiochem, La Jolla CA) for 1 h at 37°C. Biotinylated MUC1 was recovered by elution of the immunoprecipitates for 2 min at 90°C in 80  $\mu$ l 1% SDS in HBS and incubation with 30  $\mu$ l ImmunoPure Immobilized Avidin (Pierce) after addition of 0.8 ml HBS. After overnight rotation at 4°C, the avidin-conjugated beads were washed with 1 ml each: 1% Triton X-100 in HBS and HBS. The biotinylated MUC1 was recovered by heating for 3.5 min at 90°C in 50  $\mu$ l Laemmli SDS-sample buffer containing fresh 0.14 M  $\beta$ -mercaptoethanol (Laemmli, 1970). Samples were subjected to SDS-PAGE (all reagents from Bio-Rad, Richmond, CA) on 3–15% acrylamide gradient gels, and radioactive protein bands were imaged and quantitated from the dried gel using a phosphorimager (Bio-Rad). In some instances, fluorography of gels was carried out using BioMax MR film (Eastman Kodak, Rochester, NY).

### Endocytosis Assay for MUC1

Confluent cultures of MUC1-expressing CHO or ldID cells in Falcon six-well dishes (35-mm wells; Becton Dickinson Labware, Franklin Lakes, NJ) were pulse-labeled with [<sup>35</sup>S]Met/Cys for 30 min and chased for 90 min before biotinylation of cell surface proteins on ice (described above). Where indicated, GalNAc, with or without Gal, was added to the culture media throughout the radiolabeling pro-

tol. Cells in six-well dishes were rapidly warmed to 37°C on a metal plate in a Precision (Winchester, VA) model 66566 circulating water bath by the addition of prewarmed HEPES-buffered MEM (20 mM HEPES-NaOH, pH 7.4, 0.6% BSA, 4 mM NaHCO<sub>3</sub>), incubated to allow endocytosis for 1–30 min and then rapidly cooled on a metal plate on ice by two quick washes with ice-cold PBS. Where indicated, 0.45 M sucrose was included in the culture media to inhibit clathrin-mediated endocytosis (Hansen *et al.*, 1993). Biotin remaining at the cell surface was stripped by three 20-min incubations with 1 ml ice-cold 100 mM sodium 2-mercaptoethanesulfonic acid (MESNA) in 50 mM Trizma-HCl, pH 8.6, 100 mM NaCl, 1 mM EDTA, and 0.2% BSA, and residual MESNA was quenched by a 10-min incubation with ice-cold 120 mM iodoacetic acid in PBS. The internalized biotinylated MUC1 was recovered from cell extracts as described above. The total biotinylated MUC1 was determined for each sugar condition on separate six-well dishes by excluding the MESNA and iodoacetic acid washes. Cells representing the zero time point of endocytosis were incubated in ice-cold HEPES-buffered MEM on ice for 10 min before washing. Percent internalization of MUC1 was calculated by dividing the amount of biotinylated [<sup>35</sup>S]MUC1 remaining after MESNA treatment by the amount of biotinylated [<sup>35</sup>S]MUC1 recovered without MESNA treatment at each time point. Background values obtained at  $t = 0$  were subtracted from each time point and were typically 1–5% of total MUC1. Data are presented for individual representative experiments as means  $\pm$  SD for triplicate samples, allowing for error propagation. Data calculated for combined experiments are presented as the means  $\pm$  SEM.

### Endocytosis Assay for the Polymeric Immunoglobulin Receptor

Endocytosis of the polymeric immunoglobulin receptor (pIgR) in Id1D cells was determined exactly as described for MUC1 above, except that samples were immunoprecipitated using a sheep antibody directed against the luminal domain of pIgR (5 $\alpha$ S).

### Assay for Fluid Phase Endocytosis

Confluent cultures of CHO or Id1D cells expressing MUC1 in 24-well plastic dishes (15-mm wells; Costar, Cambridge, MA) were incubated for 2 h with 1 mM GalNAc, with or without 0.1 mM Gal as indicated, to mimic the conditions for radiolabeling and endocytosis of MUC1. Cells were moved to ice and washed once with cold HEPES-buffered MEM before addition of prewarmed media (with or without 0.45 M sucrose as indicated) containing horseradish peroxidase (HRP type II, Sigma) at 1 mg ml<sup>-1</sup> and incubated at 37°C for varying times. Cells were rapidly chilled on ice and washed twice quickly before three 10-min washes with HEPES-buffered MEM and a final rinse with PBS. Cells for the zero time point were incubated on ice with media containing HRP for 15 min. Cells were solubilized at room temperature with 0.2 ml of 60 mM *n*-octyl  $\beta$ -D-glucopyranoside and 0.1% SDS in HEPES-buffered saline for 20 min and assayed for peroxidase activity using tetramethylbenzidine dihydrochloride (Sigma) as described by the manufacturer. Activity is reported as the means  $\pm$  SD of triplicate samples.

### Expression of Proteins from Recombinant Adenoviruses

The cDNA for pIgR was subcloned into the pAdlox vector and a recombinant adenovirus (AV-pIgR) generated as described in Hardy *et al.* (1997). A recombinant adenovirus encoding mutant K44A dynamin-1 with an HA epitope tag (AV-K44A) was prepared as described previously (Altschuler *et al.*, 1998). Expression of dynamin from this virus requires coexpression of a tetracycline-repressible transactivating protein encoded by a different adenovirus (AV-TA). Using this system, dynamin expression can be completely blocked by including low levels of doxycycline (DOX; 20 ng/ml) in

the postinfection medium. Because initial experiments showed poor infection of CHO cells by adenovirus, a clonal line of MUC1-expressing CHO or Id1D cells stably transfected with hCAR (Bergelson *et al.*, 1997) was used for these studies. Confluent cultures of these cells were washed once with PBS and incubated with AV-TA with or without AV-K44A in 0.8 ml PBS (without calcium) for 6-well dishes or AV-pIgR in 0.3 ml PBS (without calcium) for 24-well dishes (multiplicity of infection  $\sim$  200). After 2 h at 37°C, virus was removed, and cells were washed once with 1 ml of normal culture media and incubated overnight at 37°C in the same media. Controls for the K44A dynamin expression were either cells infected with only AV-TA or cells infected with both viruses but subsequently incubated with DOX. The following day, endocytosis assays were performed as described above. Inhibition of K44A expression by DOX was confirmed by Western blot analysis of cell extracts using the mouse anti-HA monoclonal antibody 12CAS (BabCO, Richmond, CA).

### Determination of MUC1 Half-life

CHO and Id1D cells expressing MUC1 were pulse-labeled for 30 min with [<sup>35</sup>S]Met/Cys and chased in normal media for 90 min as described above. Where indicated, GalNAc with or without Gal were added to the culture media throughout the radiolabeling protocol. Cells were returned to culture for either 0 or longer times (3.5–20 h) before solubilization, immunoprecipitation, and recovery of [<sup>35</sup>S]MUC1 for SDS-PAGE and phosphorimager analysis. The half-life of MUC1 was calculated from the levels of radioactivity using the formula  $t_{1/2} = 0.693/k_d$ .

### Immunogold Labeling of Ultrathin Cryosections

CHO cells expressing MUC1 were cultured on 10-cm plastic dishes as described above. The cells were rinsed once with Dulbecco's PBS (DPBS), fixed 30 min at room temperature with 1.0% (vol/vol) glutaraldehyde and 2% (wt/vol) paraformaldehyde in DPBS, gently scraped from the dish with a flexible cell scraper, and pelleted in a microfuge at 100  $\times$  g for 5 min at room temperature. The cell pellet was resuspended in an equal volume of 3% gelatin (200 bloom; Sigma) in DPBS, incubated for 10 min at 37°C, and then placed on ice for 10 min to harden the gelatin. The gelatin cell plug was cut into 0.5- to 1.0-mm<sup>2</sup> cubes, and the cubes were incubated overnight at 4°C in 1.8 M sucrose and 20% (wt/vol) polyvinylpyrrolidone (*M<sub>w</sub>*, 10,000). The cubes were mounted on cryo-stubs and frozen in liquid nitrogen. Cryosectioning was performed at  $-110^\circ\text{C}$  in a Leica (Deerfield, IL) Ultracut E ultramicrotome with a model type FCS cryochamber attachment. The sections, collected on drops of sucrose, were transferred to butvar-coated nickel grids. Incubations were performed by inverting the grids on drops of the appropriate solution. The sections were incubated for 15 min in DPBS, washed three times 5 min each with 0.15% (wt/vol) glycine and 0.5% (wt/vol) BSA dissolved in DPBS (buffer 1), and then incubated for 20 min with 10% (vol/vol) goat serum diluted in buffer 1. The sections were incubated with VU-3-C6 anti-MUC1 antibody (ascites diluted 1:100 in buffer 1) for 60 min at room temperature, washed three times 5 min each with buffer 1 and then incubated with protein A-5 nm colloidal gold (purchased from Dr. Jan Slot, Utrecht University, Netherlands) diluted in buffer 1 for 30 min at room temperature. The sections were washed three times for 5 min each with buffer 1, washed with DPBS, fixed with 2.5% (vol/vol) glutaraldehyde (in PBS) for 5 min, rinsed with DPBS and then water, stained with 2% (wt/vol) neutral uranyl acetate, 4% (wt/vol) aqueous uranyl acetate, and then embedded in 1.2% (wt/vol) methylcellulose. Sections were viewed at 80–100 kV in a Jeol 100CX electron microscope (Peabody, MA).

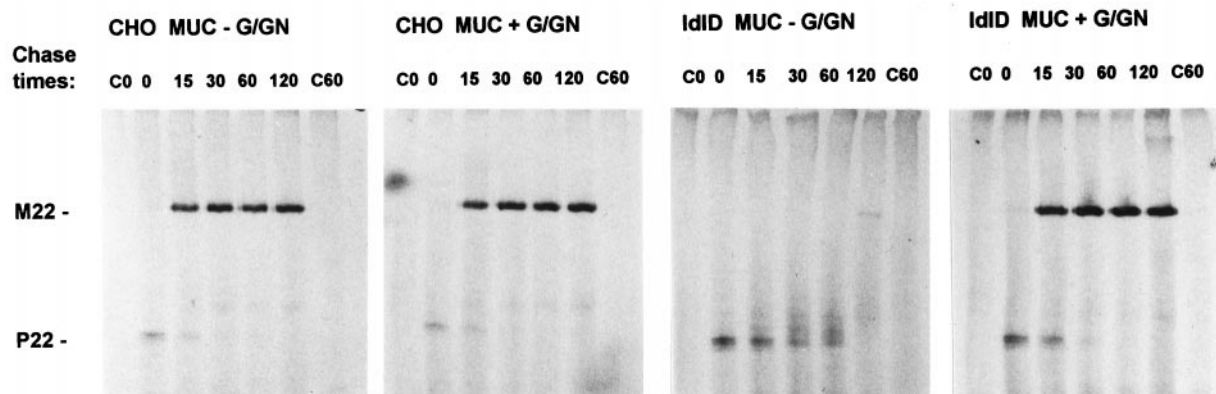


**Figure 1.** MUC1 maturation in IdID cells is rescued by Gal and GalNAc. CHO and IdID cells expressing human MUC1 were pulse labeled with [ $^{35}$ S]Met/Cys for 15 min and chased for 0–120 min. Where indicated, both 100  $\mu$ M Gal and 1000  $\mu$ M GalNAc (+G/GN) were included in the starvation, pulse and chase media. MUC1 was immunoprecipitated from cell extracts and subjected to SDS-PAGE on a 3–10% polyacrylamide gradient gel before fluorography of the dried gel. C0 and C60 in each panel show immunoprecipitates from nontransfected control cells, which were labeled and then chased for 0 and 60 min, respectively. M22 (~250 kDa) and P22 (130 kDa) denote the positions of the mature and propeptide forms of the recombinant MUC1 with 22 tandem repeats, respectively.

## RESULTS

### Cell Surface Expression of MUC1 in Normal and Glycosylation-Defective CHO Cells

When CHO cells expressing MUC1 with 22 tandem repeats are pulsed with [ $^{35}$ S]Met/Cys for 15 min and chased for varying times, the immature propeptide (P22) present at the earliest chase time ( $t = 0$ ) is rapidly processed to its fully mature form (M22;  $M_r \sim 250,000$ ) in just 15 min (Figure 1). By contrast, the majority of labeled MUC1 synthesized by IdID cells, which are defective in the synthesis of UDP-Gal (Figure 1, labeled G) and UDP-GalNAc (Figure 1, labeled GN), remains as the propeptide (P22;  $M_r \sim 130,000$ ) during the chase period and produces only a trace of mature MUC1 (–G/GN). However, addition of 100  $\mu$ M Gal and 1000  $\mu$ M GalNAc (+G/GN) to the media rescues this maturation process in IdID cells while having no adverse effect on MUC1 synthesis in CHO cells. No forms of [ $^{35}$ S]MUC1 resulting from any of the culture conditions were found in the media (unpublished observations). Comparison of the band intensities in this pulse–chase experiment also indicates that the majority of newly synthesized MUC1 is degraded in IdID cells in the absence of normal glycosylation ( $t_{1/2} \sim 30$  min). This fate is in contrast to other heavily O-glycosylated proteins synthesized in IdID cells, which either accumulate as an immature form or are released into the cell media (Kozarsky *et al.*, 1988a,b; Zanni *et al.*, 1989; Remaley *et al.*, 1991).

Because CHO cells lack the core 2  $\beta$ -1,6-GlcNAc transferase required for synthesis of branched O-glycans (Bierhuizen *et al.*, 1994), only the unbranched mucin-type O-glycans (sialylated Gal $\beta$ 1,3GalNAc-Ser/Thr) are present on the CHO MUC1. To determine if addition of truncated glycans (sialylated GalNAc-Ser/Thr) on MUC1 is sufficient to stabilize MUC1 in IdID cells, we expressed [ $^{35}$ S]MUC1 in the presence of varying levels of GalNAc (50–500  $\mu$ M); half of each immunoprecipitate was treated with neuraminidase before SDS-PAGE to assess sialylation (Figure 2). The results indicate that increasing levels of GalNAc in the IdID cell media results in both increased levels of MUC1 and a de-

creased mobility for MUC1 on SDS-gels consistent with increasing numbers of O-glycans on each molecule. However, MUC1 with truncated O-glycans migrates as a much more heterogenous band on SDS gels than fully glycosylated MUC1 (compare with CHO MUC control and IdID MUC + Gal and GalNAc in Figure 2), consistent with previous reports for undersialylated MUC1 (Litvinov and Hilkens, 1993; Poland *et al.*, 1997). Unlike most glycoproteins, sialylation of MUC1 results in faster rather than slower mobility on SDS gels, and we find that neuraminidase treatment of all forms of MUC1 decreases its mobility. Removal of sialic acid from the MUC1 with truncated O-glycans also decreases its heterogeneity and confirms our conclusion that the number of O-glycans on the protein (based on higher molecular weight) correlates with the concentration of GalNAc in the media. Thus, increasing numbers of even truncated O-glycans on MUC1 increase its stability.

To determine if this increased stability reflects increased surface expression of the MUC1, metabolically labeled cells were biotinylated with a membrane-impermeant reagent (sulfo-NHS-SS-biotin) and biotinylated [ $^{35}$ S]MUC1 was recovered from the total immunoprecipitate with avidin-conjugated beads and analyzed by SDS-PAGE. We found that MUC1 with truncated O-glycans is expressed at the cell surface, and increased numbers of O-glycans correlate with increased levels of surface expression (unpublished observations). This effect was more carefully analyzed by comparing the kinetics of fully glycosylated and underglycosylated MUC1 delivery to the cell surface (Figure 3). CHO or IdID cells expressing MUC1 were starved, pulse-labeled, and chased for 0–120 min in the presence of GalNAc, with or without Gal as indicated. After the chase period, cells were biotinylated on ice and surface [ $^{35}$ S]MUC1 was recovered for SDS-PAGE and analysis with a phosphorimager. The kinetics of surface delivery of mature MUC1 synthesized in CHO cells and IdID cells (+G/GN) were similar. The slight lag in appearance of normal MUC1 in IdID cells (both G/GN,  $t_{1/2} = 35$  min for maximal surface expression), when compared with MUC1 synthesized in CHO cells ( $t_{1/2} = 25$  min),

	ldID MUC						CHO MUC			
[ $\mu$ M Gal]	0	0	0	0	0	100	0	100		
[ $\mu$ M GalNAc]	0	50	75	100	500	1000	0	1000		
N'ase	-	+	-	+	-	+	-	+	-	+

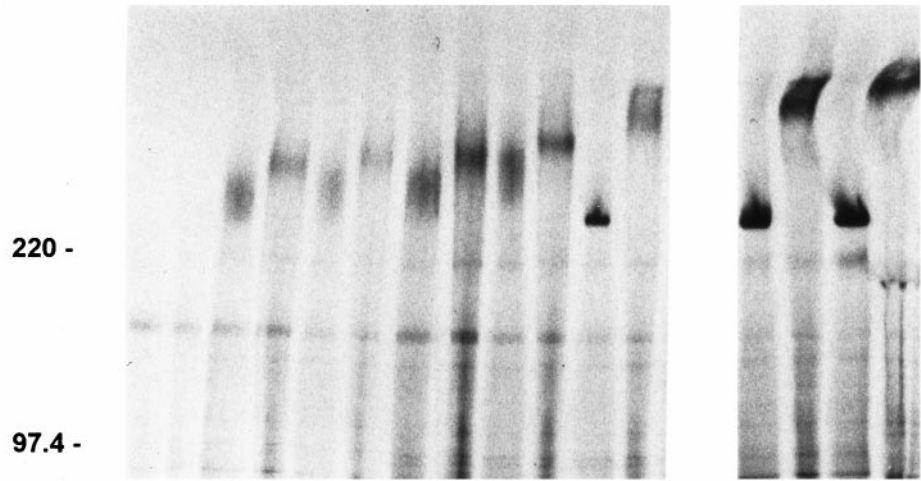


**Figure 2.** Truncated O-glycans on MUC1 can rescue its surface expression in ldID cells. Both CHO and ldID cells expressing MUC1 were pulsed with [ $^{35}$ S]Met/Cys for 15 min and chased for 90 min. Varying levels of Gal and GalNAc were included in the starvation, pulse, and chase media as indicated. Immunoprecipitates of MUC1 from cell extracts were divided in half and incubated with or without neuraminidase. Numbers to the left of the gel correspond to the mobility of the molecular weight standards in kilodaltons. All samples were subjected to SDS-PAGE and fluorography.

is likely due to a delay in the synthesis of UDP-Gal/GalNAc by an alternative pathway. In addition, the kinetics of surface delivery for underglycosylated MUC1 (+1000GN or +100GN; Figure 3) were similar to that of mature MUC1 in ldID cells; however, the level of MUC1 found at the cell surface under these conditions was markedly lower (60 and 10%, respectively). Virtually no MUC1 was found on the plasma membrane of ldID cells grown in the absence of Gal and GalNAc, consistent with our earlier observation that this form of MUC1 was rapidly degraded (Figures 1 and 2). Thus, the cumulative data indicate that MUC1 stability and surface expression are absolutely dependent on the addition of O-linked glycans, and increased size and number of O-glycans correlate with increased levels of cell surface expression.

#### MUC1 Internalization Is Affected by Glycosylation

The reduced levels of underglycosylated MUC1 found at the cell surface could be due either to decreased delivery to the cell surface or to more rapid internalization from the plasma membrane. To test whether underglycosylation of MUC1 would affect its endocytosis, we developed an assay to measure MUC1 internalization. CHO and ldID cells expressing MUC1 were starved for Met/Cys, pulsed-labeled with [ $^{35}$ S]Met/Cys for 30 min and chased for 90 min in the presence of GalNAc, with or without Gal, before chilling the cells and biotinylating the cell surface with sulfo-NHS-SS-biotin. This chase period is sufficient to deliver both underglycosylated and mature newly synthesized MUC1 to the cell surface (see Figure 3). Internalization of [ $^{35}$ S]MUC1 was initiated by rapid warming of the cells to 37°C for 15 or 30 min. At each time point, vesicular traffic was stopped by rapidly cooling the cells on ice. Biotin remaining on cell surface proteins was removed with the membrane-impermeant reducing agent MESNA. Internalized biotinylated [ $^{35}$ S]MUC1 (protected from MESNA) was recovered after

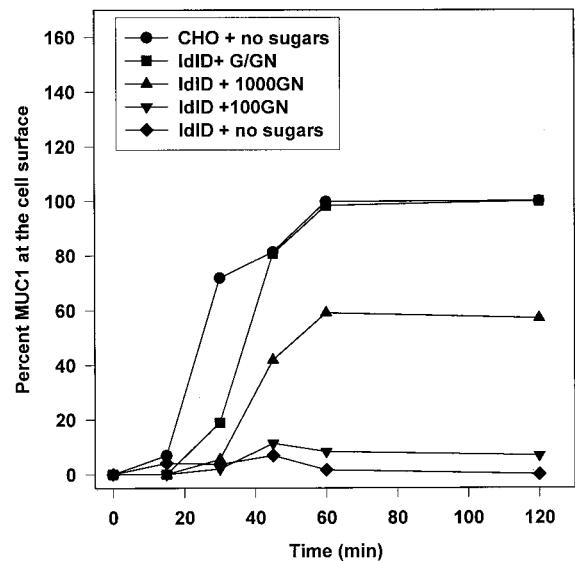


**Figure 3.** MUC1 with truncated O-glycans reaches the cell surface with normal kinetics. Both CHO and ldID cells expressing MUC1 were pulsed with [ $^{35}$ S]Met/Cys for 15 min and chased for the times indicated before biotinylation of the cell surface. Varying levels of Gal and GalNAc were included in the starvation, pulse, and chase media as indicated (100  $\mu$ M GalNAc, +100GN; 1000  $\mu$ M GalNAc, +1000GN; 1000  $\mu$ M GalNAc and 100  $\mu$ M Gal, +G/GN). Biotinylated [ $^{35}$ S]MUC1 was recovered with avidin-conjugated beads from the immunoprecipitates and subjected to SDS-PAGE for analysis of radioactive bands with a Bio-Rad phosphorimager system. Cell surface MUC1 levels in ldID samples were normalized to the maximal level of cell surface [ $^{35}$ S]MUC1 synthesized in ldID cells in the presence of both Gal and GalNAc (+G/GN). The absolute levels of MUC1 expression in CHO and ldID cells (+G/GN) are comparable (see Figure 5B).

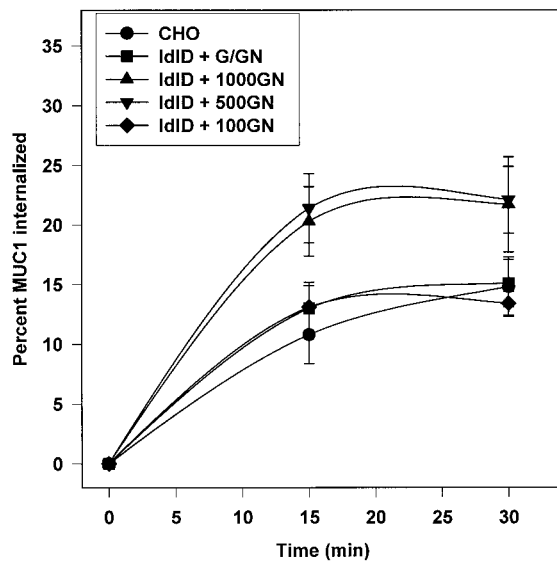


**Figure 4.** MUC1 internalization from the cell surface is affected by its glycosylation state. CHO and IdID cells expressing MUC1 were pulse labeled for 30 min and chased for 90 min before cell surface biotinylation on ice as described in MATERIALS AND METHODS. Varying levels of Gal (G, 100  $\mu$ M) and GalNAc (GN, 100, 500, or 1000  $\mu$ M) were included in the starvation, pulse and chase media as indicated. Cells were rapidly warmed to 37°C for the indicated times to allow internalization of surface MUC1 and rapidly cooled on ice, and remaining cell surface biotin was stripped with MESNA. Some samples were not treated with MESNA in order to determine the total amount of biotinylated MUC1 at  $t = 0$ . Internalized biotinylated MUC1 was recovered from the MUC1 immunoprecipitates with avidin-conjugated beads, and [ $^{35}$ S]MUC1 was analyzed after SDS-PAGE using a phosphorimager. Data are plotted as the percent of total biotinylated [ $^{35}$ S]MUC1 internalized at each time point and are presented as means  $\pm$  SD of triplicate samples. Similar results were obtained in six experiments.

cell lysis by incubation of immunoprecipitated MUC1 with avidin-conjugated beads. The percent of surface MUC1 internalized at a given time point was calculated by comparison to control plates of cells not washed with MESNA. As shown in Figure 4, the level of internalized [ $^{35}$ S]MUC1 was near maximal at 15 min for all glycosylated forms of MUC1. Interestingly, the level of underglycosylated MUC1 (synthesized in IdID + 500GN or + 1000GN) that was internalized over this time period was approximately twice that of mature MUC1 (synthesized in CHO cells or in IdID cells + G/GN). However, the intracellular accumulation of poorly glycosylated [ $^{35}$ S]MUC1 (synthesized in IdID + 100GN) was not enhanced, indicating that there is a threshold of reactivity associated with the number of truncated O-glycans on the MUC1.

This increased intracellular accumulation of underglycosylated MUC1 could reflect an increased initial rate of endocytosis, a decreased recycling rate, or both. We therefore compared the initial rate of endocytosis of surface biotinylated underglycosylated and mature [ $^{35}$ S]MUC1 in IdID cells (Figure 5). Endocytosis of both mature (G+GN) and underglycosylated (1000GN) MUC1 was evident within 1 min and proceeded in a linear manner for at least 7 min. However,

we consistently found a twofold greater initial rate of endocytosis for the MUC1 with truncated O-glycans, which was consistent with the levels of MUC1 accumulating after 15–30 min (Figure 4). Although it is possible that underglycosylated MUC1 with smaller glycans could exhibit higher levels of biotinylation that could affect its structure and endocytosis, this is unlikely since the repetitive sequences with the most O-glycans do not contain lysine residues. Although we attempted to modify our assay to compare the initial rate of return of internalized MUC1 to the cell surface (recycling), we did not obtain reproducible results using this approach.

#### *Increased Internalization Does Not Lead to Increased Degradation of MUC1*

One explanation for the increased internalization of underglycosylated MUC1 might be recognition by quality control machinery at the cell surface leading to MUC1 retrieval and degradation. To determine whether enhanced internalization is linked to increased degradation of underglycosylated MUC1, the half-life of MUC1 in CHO and IdID cells grown under various culture conditions was determined as described in MATERIALS AND METHODS. As shown in Table 1, the MUC1 synthesized in IdID cells in the presence of 1000  $\mu$ M GalNAc, with or without 100  $\mu$ M Gal, had the same half-life as the mature MUC1 synthesized in CHO cells. The degradation of MUC1 in CHO cells was blocked by including an inhibitor of lysosomal acidification (the weak base ammonium chloride) in the culture media (unpublished observations), but not by the presence of a proteasome inhibitor (the peptide aldehyde MG-132) (Rock *et al.*, 1994). Because MUC1 in these cells is not shed into the media (unpublished observations), this would indicate that MUC1 turns over by degradation in lysosomes. Thus, increased intracellular accumulation of underglycosylated MUC1 in IdID cells is the direct result of increased endocytosis and is not linked to increased degradation.

#### *MUC1 Is Internalized by Dynamin-dependent, Clathrin-mediated Endocytosis*

To determine whether normal and enhanced internalization of MUC1 proceed via the same mechanism or by different pathways, endocytosis of mature and underglycosylated MUC1 was measured under conditions that are known to inhibit clathrin-mediated endocytosis. As shown in Figure 6A, endocytosis of normal MUC1 in CHO cells and underglycosylated MUC1 in IdID cells (synthesized in the presence of 1000  $\mu$ M GalNAc) was completely inhibited by hypertonic media. By contrast, fluid phase endocytosis of HRP, which proceeds through both clathrin-mediated and clathrin-independent pathways was inhibited only 50% (Figure 6B). Thus, the increased internalization of MUC1 resulting from its altered glycosylation does not occur via an alternate route but is likely to result directly from increased clathrin-mediated endocytosis of MUC1.

Additional experiments were carried out to confirm that MUC1 internalization occurs via clathrin-coated pits. Because the actual budding of clathrin-coated endocytic vesicles requires the 100-kDa GTPase dynamin-1, CHO cells expressing MUC1 were infected with recombinant adenovirus encoding the dominant-negative mutant (K44A) of dynamin-1 (Altschuler *et al.*, 1998). Expression of K44A dy-

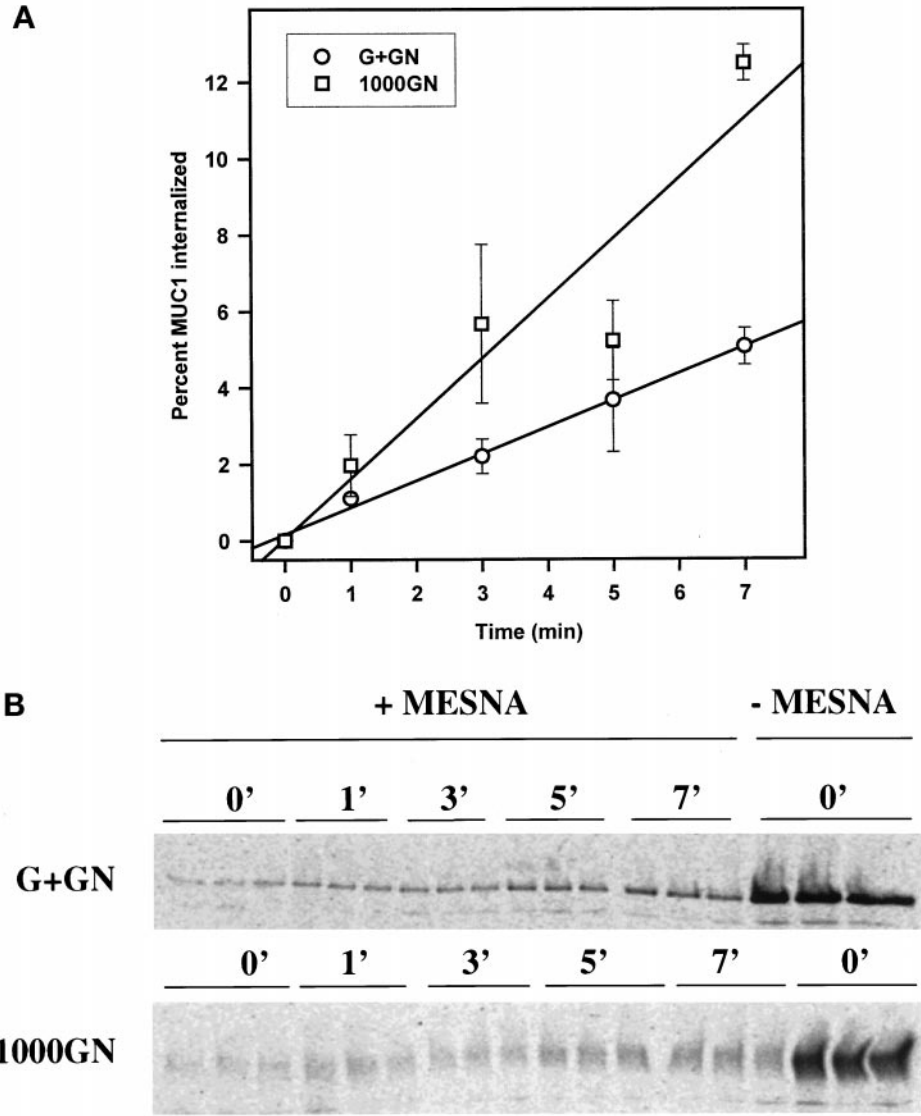


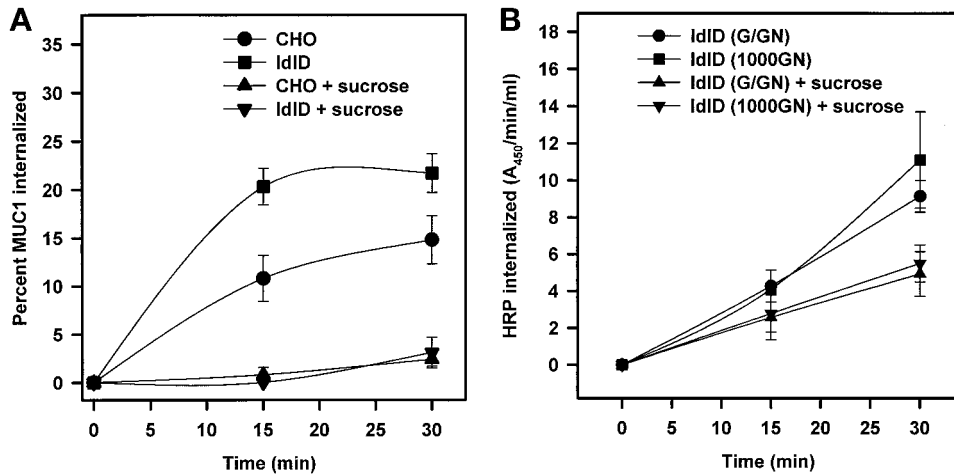
**Figure 5.** The initial rate of MUC1 endocytosis is enhanced by altered glycosylation. (A) The rate of endocytosis of [<sup>35</sup>S]MUC1 in Id1D cells, synthesized in the presence of either 1000 μM GalNAc (1000GN) with or without 100 μM Gal (G+GN), was characterized as described in MATERIALS AND METHODS and the legend to Figure 4. The mean of the percent endocytosis ± SEM for each time point for three experiments is shown. By paired Student's *t* test analysis, only the data at 7 min was significantly different (*p* = 0.015) between the two sugar conditions. Regression lines are drawn for each data set and indicate a 2.2-fold difference in the rate of endocytosis (*p* < 0.05). (B) A representative SDS-gel pattern for internalized [<sup>35</sup>S]MUC1 from a single experiment is shown, where *n* = 3 at each time point.

namin in this system is under control of the tetracycline operon and can be blocked by inclusion of DOX in the postinfection medium (Figure 7C). As shown in Figure 7A, expression of dominant-negative dynamin K44A inhibits the internalization of MUC1 by ~ 80%, whereas fluid phase endocytosis of HRP is inhibited only 20% (Figure 7B). This inhibition of MUC1 endocytosis was directly due to the expression of the mutant dynamin, because normal endocytosis levels were observed either in cells infected only with AV-TA or in cells cultured in the presence of DOX. Finally, ultrathin cryosections of CHO cells expressing MUC1 were stained with the anti-MUC1 antibody VU-3-C6 and protein A-conjugated 5 nm gold to assess the subcellular localization of the MUC1 in these cells. Consistent with our biochemical data, MUC1 was found evenly distributed on the plasma membrane, including the microvillar protrusions (Figure 8, A and C). Most notably, MUC1 was observed in both coated pits (Figure 8B) and coated vesicles (Figure 8, A and C),

**Table 1.** Enhanced endocytosis of MUC1 is not linked to increased degradation

Cells and culture conditions	Half-life (h)
CHO MUC (n = 8)	29.9 ± 6.6
Id1D MUC + G/GN (n = 5)	26.1 ± 3.5
Id1D MUC + 1000GN (n = 5)	20.7 ± 5.2

Values are means ± SEM. CHO and Id1D cells were pulse labeled for 30 min and chased for 90 min as described in MATERIALS AND METHODS. Where indicated, GalNAc, with or without Gal, were included in the starvation, pulse, and chase media (abbreviations are described in legend to Figs. 1–6). Cells were either solubilized immediately or returned to culture; immunoprecipitates of [<sup>35</sup>S]MUC1 were subjected to SDS-PAGE and phosphorimager analysis. The half-life of [<sup>35</sup>S]MUC1 was calculated as described in MATERIALS AND METHODS.



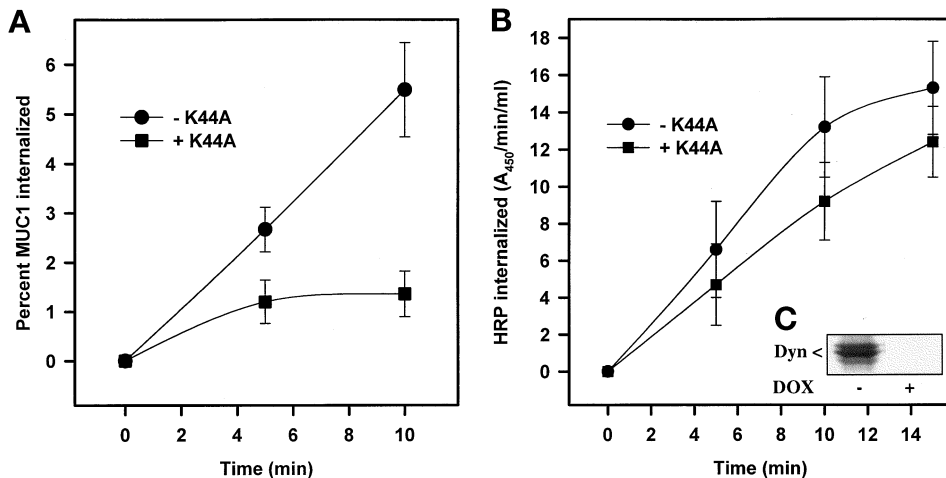
without 100  $\mu$ M Gal. Endocytosis of the fluid phase marker HRP, carried out in the presence (+ sucrose) or absence of hypertonic media, was determined as described in MATERIALS AND METHODS.

consistent with clathrin-mediated endocytosis of MUC1; however, MUC1 was not found in any noncoated pits on the plasma membrane. In addition, MUC1 was also found in Golgi-associated vesicles (Figure 8D), although there is no way to know if this is within the recycling pathway or the pathway of de novo synthesis. Together, these experiments demonstrate that internalization of both mature and underglycosylated MUC1 is mediated by the classical clathrin- and dynamin-dependent endocytic machinery.

**Enhanced MUC1 Endocytosis Does Not Affect Internalization of pIgR**

To confirm that the effects we observed on MUC1 internalization were due to its own altered glycosylation and not to

changes in the integrity of the endocytic pathway of ldlID cells, we measured the internalization rate of a control receptor, pIgR, in stably transfected ldlID cells grown under these same culture conditions. Internalization of pIgR in ldlID cells was measured using the identical protocol followed for MUC1. Although the internalization rate for pIgR was considerably faster than that of MUC1 (20% within 1 min), there was no difference in internalization of [<sup>35</sup>S]pIgR synthesized in ldlID cells in the presence of GalNAc, with or without Gal (Figure 9A). Similarly, when we examined the rate of internalization of <sup>125</sup>I-labeled dimeric IgA prebound to surface pIgR on these ldlID cells, we did not find any difference in the initial rate of uptake (Figure 9C). In addition, the level of [<sup>35</sup>S]pIgR synthesis was identical under the



seven ( $t = 10$  min) experiments is shown. By paired Student's  $t$  test analysis, MUC1 endocytosis under the two conditions was significantly different at both time points ( $p \leq 0.01$ ). (B) CHO cells expressing MUC1 and infected as described above for (A) were grown overnight with (-K44A) or without (+K44A) DOX in the media before assay of HRP uptake as described in MATERIALS AND METHODS. Data are a representative experiment with the mean  $\pm$  SD of triplicate samples at each time point. (C) Identical aliquots of adenoviral-infected cells from the experiment described in (B) were grown overnight with (+DOX) or without (-DOX) doxycycline and subjected to Western blot analysis with an anti-HA tag antibody to visualize HA-tagged dynamin-1 (K44A) under the two culture conditions.

**Figure 6.** MUC1 internalization is inhibited by hypertonic media. (A) CHO and ldlID cells expressing MUC1 were pulse labeled for 30 min and chased for 90 min. GalNAc (1000  $\mu$ M) was included in the starvation, pulse, and chase media for the ldlID cells. After biotinylation on ice, cells were rapidly warmed to 37°C in the presence of normal or hypertonic media (supplemented with 0.45 M sucrose) for the indicated times. The level of internalized MUC1 was determined as described in MATERIALS AND METHODS and the legend to Figure 4. (B) ldlID cells expressing MUC1 were preincubated for 2 h in media with 1000  $\mu$ M GalNAc, with or

**Figure 7.** MUC1 internalization is dynamin dependent. (A) Clonal CHO cells expressing both MUC1 and hCAR were infected with adenoviruses expressing the tetracycline-repressible transactivating protein (AV-TA) and the dominant-negative mutant of dynamin-1 (+K44A, ■). Controls (-K44A, ●) for the experiments were either cells infected with only AV-TA or cells infected with both viruses but incubated subsequently with the tetracycline analogue doxycycline (DOX) in the media. The following day, [<sup>35</sup>S]MUC1 endocytosis was determined as described in MATERIALS AND METHODS and the legend to Figure 5. The mean of the percent endocytosis  $\pm$  SEM for each time point for six ( $t = 5$  min) and

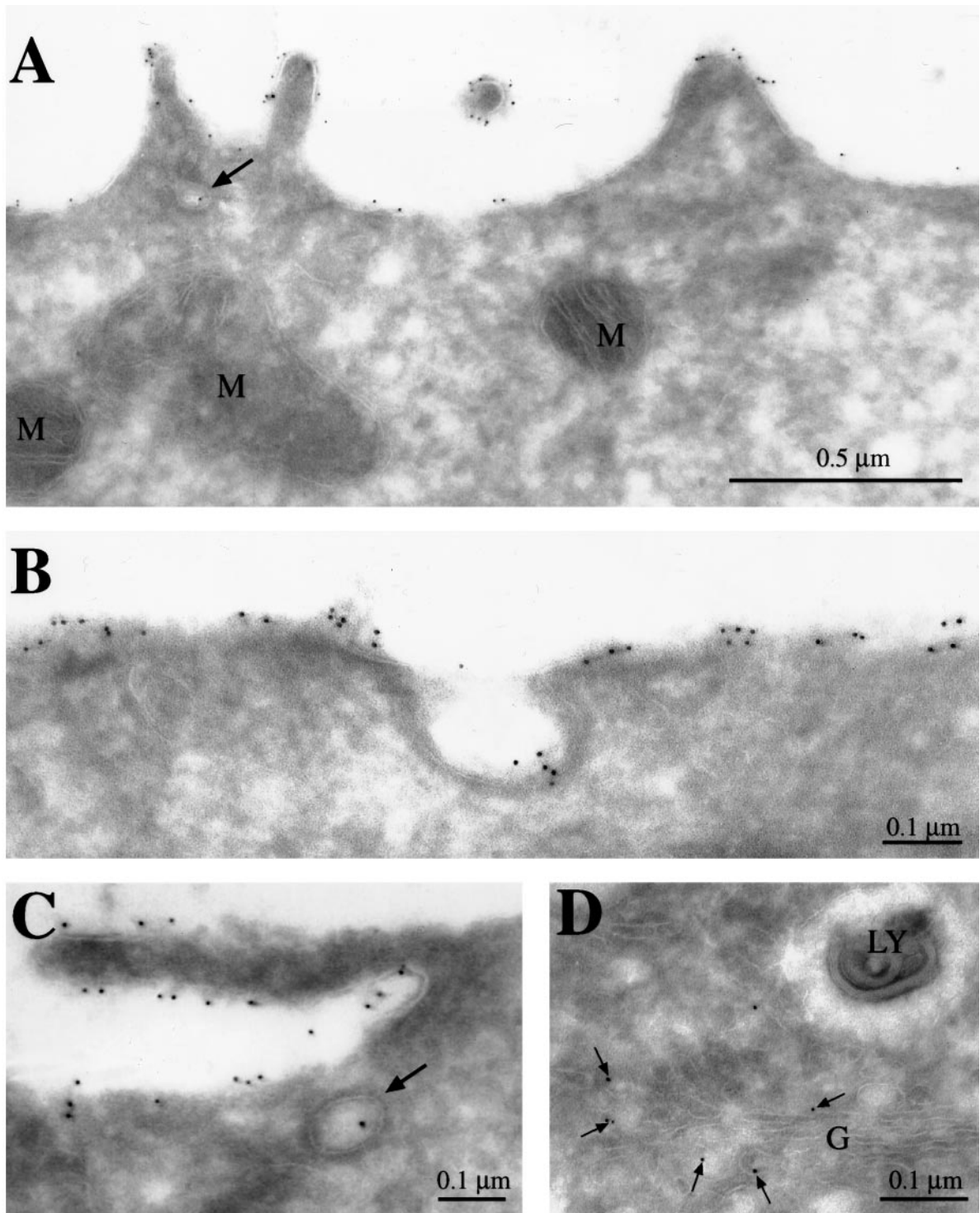


**Figure 8.** Distribution of MUC1 in transfected CHO cells. Ultrathin cryosections of CHO cells expressing MUC1 were sequentially incubated with anti-MUC1 monoclonal antibody VU-3-C6 and protein A conjugated to 5 nm colloidal gold. MUC1 was observed at the cell surface (A–C), in coated pits (B), and in coated invaginations and coated vesicles (marked with arrows in A and C, respectively). (D) MUC1 was also found in Golgi-associated vesicles. G, Golgi; LY, lysosome; M, mitochondria.

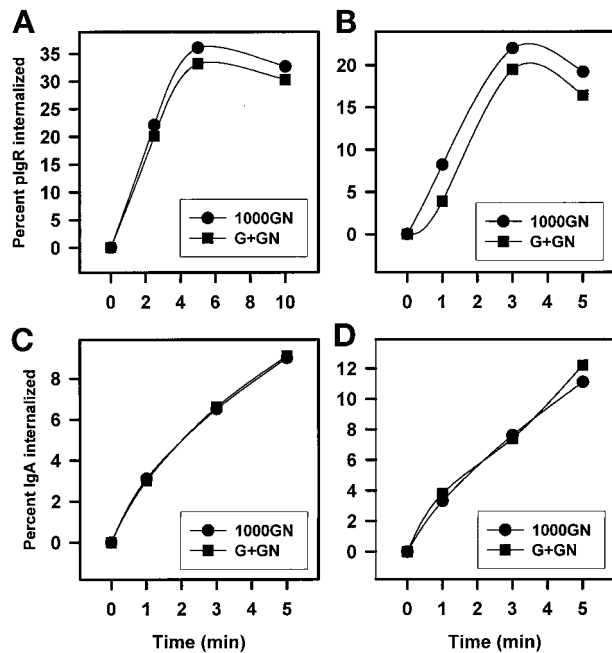


**Figure 9.** The endocytosis of pIgR in ldlD cells is unaffected by changes in glycosylation conditions or the presence of MUC1. The endocytosis of [ $^{35}$ S]pIgR synthesized in the presence of either 1000  $\mu$ M GalNAc, with (●) or without (■) 100  $\mu$ M Gal, in ldlD cells with (B) or without (A) MUC1 coexpression was characterized as described in MATERIALS AND METHODS. Endocytosis of dimeric  $^{125}$ I-labeled IgA prebound to pIgR in ldlD cell with (D) or without (C) coexpression of MUC1 was carried out after preincubation for 2 h with 1000  $\mu$ M GalNAc, with (●) or without (■) 100  $\mu$ M Gal. Points are the mean of triplicate samples for representative experiments. Experiments were carried out 2–4 times with similar results. Error values at each point were <20% for both assays.

two glycosylation conditions (unpublished observations), and the extent of endocytosis in CHO and ldlD cells was similar to the kinetics described for pIgR-dependent dimeric IgA uptake in fibroblasts (Mostov *et al.*, 1986). Thus, the glycosylation-dependent stimulation of endocytosis in ldlD cells is MUC1 specific.

To determine whether enhanced clathrin-mediated endocytosis of MUC1 could affect internalization of other proteins in this pathway, pIgR endocytosis in ldlD cells was also measured in the presence of MUC1 (Figure 9, B and D). Coexpression of MUC1 and pIgR was achieved by stably transfecting ldlD cells expressing MUC1 with the adenovirus receptor hCAR; this stable cell line was then infected with AV-pIgR to obtain pIgR expression. However, when the endocytosis of either pIgR (Figure 6B) or dimeric IgA prebound to pIgR (Figure 6D) was studied in these ldlD cells expressing MUC1, there was no significant difference in either receptor or ligand internalization under the two glycosylation conditions. Endocytosis of pIgR was no different in CHO and ldlD cells in the absence of any sugar additions (unpublished observations). Thus, enhanced internalization of MUC1 apparently does not affect clathrin-mediated endocytosis of other proteins using this pathway.

## DISCUSSION

### Normal MUC1 Expression Is Dependent on O-linked Glycosylation

Glycosylation-defective ldlD cells have been used previously to characterize the role of O-linked glycans in the synthesis and stability of several secreted and plasma membrane proteins. In the absence of sugar supplements, ldlD cells secrete granulocyte macrophage colony-stimulating factor, human chorionic gonadotropin, apoprotein E, and apoprotein A-II, all devoid of O-linked glycans, with normal kinetics (Matzuk *et al.*, 1987; Zanni *et al.*, 1989; Remaley *et al.*, 1993). However, normal membrane protein expression is much more dependent on O-linked glycosylation. For example, the surface membrane expression of the respiratory syncytial virus G-protein in ldlD cells requires either N- or O-linked glycans (Wertz *et al.*, 1989), whereas the surface expression of glycoprotein (LDL) receptor (Kozarsky *et al.*, 1988a), the human interleukin 2 receptor (Kozarsky *et al.*, 1988b), decay-accelerating factor (Reddy *et al.*, 1999), and the envelope protein of Epstein-Barr virus (Kozarsky *et al.*, 1988b) all have an absolute requirement for O-linked glycosylation. In the case of the LDL receptor, decay-accelerating factor, and Epstein-Barr virus envelope protein, the proteins lacking O-linked glycans are unstable and disappear from the cell during metabolic-labeling studies after just 1 h. However, the ectodomains of these proteins appear in the cell media, consistent with cleavage of the protein adjacent to the transmembrane domains. By contrast, a form of the human interleukin 2 receptor lacking O-linked glycans is stable in the cell during metabolic-labeling studies but does not accumulate at the cell surface. However, the N-linked glycans on this aberrant receptor acquire resistance to endoglycosidase H treatment, indicating that the protein travels at least into the Golgi. This result suggests that the lack of O-linked glycans causes either retention of the receptor in the Golgi or transient surface expression followed by rapid endocytosis and intracellular accumulation. Inclusion of GalNAc in the media of ldlD cells results in O-linked glycosylation of these missorted membrane proteins and nearly normal levels of surface expression (Kozarsky *et al.*, 1988a,b; Remaley *et al.*, 1991; Reddy *et al.*, 1999).

When MUC1 is expressed in ldlD cells, only the 130-kDa precursor appears transiently before it is apparently degraded (Figure 1); because MUC1 does not appear in the media, this represents an alternative fate for a membrane protein lacking O-linked glycans. The entire MUC1 ectodomain exhibits a highly extended  $\beta$ -turn helix structure (Fontenot *et al.*, 1995) resulting from its high content of proline throughout the tandem repeats and the flanking imperfect repeats, and the absence of O-linked glycans in this domain is likely to result in the complete degradation of the protein rather than a single cleavage event. However, addition of GalNAc to the media of ldlD cells stabilizes MUC1, resulting in significant surface expression (60% of fully glycosylated MUC1) with near normal kinetics (Figure 3). Despite this efficient delivery of MUC1 with truncated glycans to the cell surface, subsequent experiments indicate that this form does accumulate within the cell, presumably by enhanced endocytosis (Figures 5 and 6).

### **MUC1 Endocytosis Is Clathrin Mediated and Dynamin Dependent**

To characterize the regulation of MUC1 endocytic trafficking in CHO cells, we first developed a sensitive biotin protection assay to follow the internalization of the de novo [<sup>35</sup>S]MUC1 synthesized with varying levels of glycosylation. Although the underglycosylated MUC1 in Id1D cells (+1000 μM GalNAc) was internalized at twice the rate of the normally glycosylated MUC1 (Figure 5), this is not a generalized effect on endocytosis of all proteins in the Id1D cells, because neither pIgR nor its ligand was endocytosed differently under the two glycosylation states (Figure 9).

This glycosylation-dependent enhancement of MUC1 endocytosis in Id1D cells (Figure 5) led us to determine whether there were alternate routes for basal and stimulated MUC1 endocytosis. Hypertonic media is known to inhibit clathrin-mediated endocytosis (Hansen *et al.*, 1993), with lesser effects on fluid phase endocytosis (Oka *et al.*, 1989), and we found that both the normal and stimulated uptake of MUC1 were completely inhibited by inclusion of hypertonic media in the endocytosis assay (Figure 6). Fluid phase endocytosis was inhibited 50% under these same conditions, which is comparable to levels of inhibition previously reported (Oka *et al.*, 1989). Thus, it appears that the altered glycosylation of MUC1 results in a direct stimulation of its endocytosis through clathrin-coated pits. The role of clathrin-mediated endocytosis in the internalization of MUC1 was confirmed by the observation that expression of the dominant-negative mutant of the GTPase dynamin-1 (K44A), which plays a direct role in the fission of deeply invaginated clathrin-coated pits (Schmid, 1997), also inhibits MUC1 endocytosis by 80% (Figure 7). By comparison, fluid phase endocytosis was inhibited only 20% by expression of dynamin-1 (K44A), comparable to inhibition levels previously reported in HeLa cells for the expression of dominant-negative dynamin-1 mutants (Damke *et al.*, 1995; Skretting *et al.*, 1999).

Most microvillar proteins are excluded from clathrin-coated pits (Bretscher *et al.*, 1980; Rodman *et al.*, 1986). The simplest explanation for this observation is that both the microvillar GPI-anchored proteins and transmembrane hydrolases lack cytoplasmic signals for endocytosis. However, MUC1 is unique because it is localized primarily on microvilli but does enter clathrin-coated pits, as shown by immunoelectron microscopy in Figure 9. This localization in clathrin-coated pits suggests that one of the seven tyrosine motifs in the MUC1 cytoplasmic domain may bind adaptors involved in recruitment of clathrin to the plasma membrane (Kirchhausen *et al.*, 1997). In fact, both the first (YGQL) and sixth (YEKV) tyrosine motif from the membrane fit the consensus sequence (YXX $\phi$ ) for binding adaptors, and characterization of their role in MUC1 endocytosis is in progress.

### **Potential Mechanisms for Stimulation of MUC1 Endocytosis**

The simplest explanation for the increased endocytosis of MUC1 with truncated O-glycans when compared with mature MUC1 is that more of the underglycosylated MUC1 can fit into a coated pit because there is less steric hindrance between MUC1 molecules. Future experiments will be directed at testing this possibility using MUC1 with larger glycans in CHO cells expressing the core 2  $\beta$ -1,6-GlcNAc

transferase. In addition, the secondary structure and length of this highly extended protein is likely to be modulated by the number and size of O-glycans (Fontenot *et al.*, 1995), which in turn could affect budding of clathrin-coated pits into coated vesicles. It is predicted that the fully extended MUC1 with 30–90 tandem repeats would be 200–500 nm long (Hilkens *et al.*, 1992), whereas the diameter of a clathrin-coated vesicle is ~150 nm. Thus, a mechanism must exist for the compaction of MUC1 within intracellular vesicles and the presence of smaller O-glycans on MUC1 should enhance this step.

We also considered the possibility that the presence of more MUC1 molecules in each clathrin-coated pit could enhance budding into vesicles by recruitment of cytoplasmic proteins regulating endocytosis. For example, there have been reports that the adaptor protein Grb2, which binds the PRD domain of dynamin through its SH3 sites (Barylko *et al.*, 1998), can also bind a phosphorylated tyrosine motif in the cytoplasmic domain of the MUC1 through its SH2 site (Pandey *et al.*, 1995). Thus, increased MUC1 accumulation within the clathrin-coated pit due to the truncated O-glycans could have the side effect of recruiting more dynamin and enhancing the rate of coated-vesicle formation. This hypothesis also would predict that clathrin-mediated endocytosis of other proteins such as pIgR, which use clathrin-mediated endocytosis, would also be enhanced when coexpressed with MUC1 under these stimulated conditions. This possibility was tested by following the endocytosis of pIgR when coexpressed with MUC1. However, culture conditions that produce enhanced endocytosis of MUC1 did not show any change in the internalization of pIgR or its ligand. Thus, the enhanced endocytosis of MUC1 resulting from its expression with truncated O-glycans is specific for MUC1 and does not seem to affect endocytosis of other proteins using the clathrin-mediated endocytosis pathway. Future experiments will be directed at understanding the regulation of MUC1 phosphorylation and whether its interaction with Grb2 might affect its entry into clathrin-coated pits.

### **MUC1 Recycles at the Cell Surface**

Litvinov and Hilkens (1993) have shown previously in ZR-75-1 human mammary carcinoma cells that endogenous MUC1 recycles at the plasma membrane with a total intracellular residence time of 66 min, and 30% of the total MUC1 is intracellular at all times. Their study followed the reappearance of mature MUC1 after neuraminidase treatment of the cell surface to produce the more slowly migrating form of the MUC1. However, we (unpublished results) and others (Ulmer and Palade, 1989; Chege and Pfeffer, 1990; Huang and Snider, 1993) have found that CHO cells do not resialylate recycling proteins after neuraminidase treatment of the cell surface. Hull *et al.* (1991) have previously shown that the rat mucin, ASGP-1, receives new O-linked glycans after its initial delivery to the cell surface, presumably by recycling through intracellular compartments. Therefore, we have confirmed MUC1 recycling in Id1D cells by following GalNAc-dependent incorporation of [<sup>3</sup>H]Gal (new O-glycans) into underglycosylated, surface-biotinylated MUC1 (Altschuler *et al.*, 1997). Because polypeptide GalNAc-transferases are found throughout the Golgi complex (Röttger *et al.*, 1998), this means that the MUC1 recycles from the cell surface through at least one of these compartments. Thus,

future experiments will further characterize the route and regulation of MUC1 recycling through the Gogi complex.

## ACKNOWLEDGMENTS

We thank Jennifer Henkel for help with the dimeric IgA endocytosis experiments; W. Geovany Ruiz for preparation of ultrathin cryosections for immunoelectron microscopy; Jeffrey M. Bergelson (Children's Hospital, Philadelphia, PA) and Robert W. Finberg (Harvard Medical School, Boston, MA) for the hCAR cDNA and anti-hCAR antibodies; John Hilkens (The Netherlands Cancer Institute, Amsterdam) for 232A1 anti-MUC1 antibody; Olivera J. Finn (University of Pittsburgh, Pittsburgh, PA) for VU-3-C6 anti-MUC1 antibody obtained from Jo Hilgers (Free University, Amsterdam, The Netherlands); and Keith Mostov (UCSF, San Francisco, CA) for the pIgR cDNA. This work was supported by fellowship DAMD17-1-97 from the Department of Defense (DOD-Army Breast Cancer Fellowship to Y.A.); National Institutes of Health grants DK51970 (to G.A.), DK54407 (to O.A.W.), and DK26012 (to R.P.H.); and the Dialysis Clinic, Inc.

## REFERENCES

Altschuler, Y., Barbas, S.M., Terlecky, L.J., Tang, K., Hardy, S., Mostov, K., and Schmid, S.L. (1998). Redundant and distinct functions for dynamin-1 and dynamin-2 isoforms. *J. Cell Biol.* *143*, 1871–1881.

Altschuler, Y., Poland, P.A., Kinlough, C.L., and Hughey, R.P. (1997). Role of endocytosis in the maturation of the membrane-associated mucin MUC1. *Mol. Biol. Cell* *8*, 301a.

Barylko, B., Binns, D., Lin, K.-M., Atkinson, M.A.L., Jameson, D.M., Yin, H.L., and Albanesi, J.P. (1998). Synergistic activation of dynamin GTPase by Grb2 and phosphoinositides. *J. Biol. Chem.* *273*, 3791–3797.

Bergelson, J.M., Cunningham, J.A., Droguett, G., Kurt-Jones, E.A., Krithivas, A., Hong, J.S., Horwitz, M.S., Crowell, R.L., and Finberg, R.W. (1997). Isolation of a common receptor for coxsackie B viruses and adenoviruses 2 and 5. *Science* *275*, 1320–1323.

Bierhuizen, M.F.A., Maemura, K., and Fukuda, M. (1994). Expression of a differentiation antigen and poly-N-acetyllactosaminyl O-glycans directed by a cloned core 2  $\beta$ -1,6-N-acetylglucosaminyltransferase. *J. Biol. Chem.* *269*, 4473–4479.

Bièche, I., Ruffet, E., Zweibaum, A., Vildé, F., Lidereau, R., and Franc, B. (1997). MUC1 mucin gene, transcripts, and protein in adenomas and papillary carcinomas of the thyroid. *Thyroid* *7*, 725–731.

Bretscher, M.S., Thomson, J.N., and Pearse, B.M.F. (1980). Coated pits act as molecular filters. *Proc. Natl. Acad. Sci. USA* *77*, 4156–4159.

Ceriani, R.L., Chan, C.M., Baratta, F.S., Ozzello, L., DeRosa, C.M., and Habif, D.V. (1992). Levels of expression of breast epithelial mucin detected by monoclonal antibody BrE-3 in breast-cancer prognosis. *Int. J. Cancer* *51*, 343–354.

Chardin, P., Camonis, J.H., Gale, N.W., Van Aelst, L., Scholessinger, J., Wigler, M.H., and Bar-Sagi, D. (1993). Human Sos1: a guanine nucleotide exchange factor for Ras that binds to GRB2. *Science* *260*, 1338–1343.

Chege, N.W., and Pfeffer, S.R. (1990). Compartmentation of the Golgi complex: Brefeldin-A distinguishes trans-Golgi cisternae from the trans-Golgi network. *J. Cell Biol.* *111*, 893–899.

Damke, H., Baba, T., van der Blik, A.M., and Schmid, S.L. (1995). Clathrin-independent pinocytosis is induced in cells overexpressing a temperature-sensitive mutant of dynamin. *J. Cell Biol.* *131*, 69–80.

Egan, S.E., Giddings, B.W., Brooks, M.W., Buday, L., Sizeland, A.M., and Weinberg, R.A. (1993). Association of Sos Ras exchange protein with Grb2 is implicated in tyrosine kinase signal transduction and transformation. *Nature* *363*, 45–51.

Fontenot, J.D., Mariappan, S.V.S., Catasti, P., Domenech, N., Finn, O.J., and Gupta, G. (1995). Structure of a tumor associated antigen containing a tandemly repeated immunodominant epitope. *J. Biomol. Struct. Dynam.* *13*, 245–260.

Gendler, S., Spicer, A.P., Lalani, E.-N., Duhig, T., Peat, N., Burchell, J., Pemberton, L., Boshell, M., and Taylor-Papadimitriou, J. (1991). Structure and biology of a carcinoma-associated mucin, MUC1. *Am. Rev. Respir. Dis.* *144*, S42–S47.

Gottardi, C.J., and Caplan, M.J. (1992). Cell surface biotinylation in the determination of epithelial membrane polarity. *J. Tissue Culture Methods* *14*, 173–180.

Hanisch, F.-G., Uhlenbruck, G., Peter-Katalinic, J., Egge, H., Dabrowski, J., and Dabrowski, U. (1989). Structures of neutral O-linked polyactosaminoglycans on human skim milk mucins. *J. Biol. Chem.* *264*, 872–883.

Hansen, S.H., Sandvig, K., and van Deurs, B. (1993). Clathrin and HA2 adaptors: effects of potassium depletion, hypertonic medium, and cytosol acidification. *J. Cell Biol.* *121*, 61–72.

Hardy, S., Kitamura, M., Harris-Stansil, T., Dai, Y., and Phipps, M.L. (1997). Construction of adenovirus vectors through Cre-*lox* recombination. *J. Virol.* *71*, 1842–1849.

Hilkens, J., Ligtenberg, M.J.L., Vox, H.L., and Litvinov, S.V. (1992). Cell membrane-associated mucins and their adhesion-modulating property. *Trends Biochem. Sci.* *17*, 359–363.

Huang, K.M., and Snider, M.D. (1993). Glycoprotein recycling to the galactosyltransferase compartment of the Golgi complex. *J. Biol. Chem.* *268*, 9302–9310.

Hull, S.R., Bright, A., Carraway, K.L., Abe, M., Hayes, D.F., and Kufe, D.W. (1989). Oligosaccharide differences in the DF3 sialomucin antigen from normal human milk and the BT-20 human breast carcinoma cell line. *Cancer Commun.* *1*, 261–267.

Hull, S.R., Sugarman, E.D., Spielman, J., and Carraway, K.L. (1991). Biosynthetic maturation of an ascites tumor cell surface sialomucin. *J. Biol. Chem.* *266*, 13580–13586.

Kingsley, D.M., Kozarsky, K.F., Hobbie, L., and Krieger, M. (1986). Reversible defects in O-linked glycosylation and LDL receptor expression in a UDP-Gal/UDP-GalNAc 4-epimerase deficient mutant. *Cell* *44*, 749–759.

Kirchhausen, T., Bonifacino, J.S., and Riezman, H. (1997). Linking cargo to vesicle formation: receptor tail interactions with coat proteins. *Curr. Opin. Cell Biol.* *9*, 488–495.

Kornfeld, S. (1987). Trafficking of lysosomal enzymes. *FASEB J.* *1*, 462–468.

Kozarsky, K., Kingsley, D., and Krieger, M. (1988a). Use of a mutant cell line to study the kinetics and function of O-linked glycosylation of low density lipoprotein receptors. *Proc. Natl. Acad. Sci. USA* *85*, 4335–4339.

Kozarsky, K.F., Call, S.M., Dower, S.K., and Krieger, M. (1988b). Abnormal intracellular sorting of O-linked carbohydrate-deficient interleukin-2 receptors. *Mol. Cell Biol.* *8*, 3357–3363.

Laemmli, U.K. (1970). Cleavage of structural proteins during the assembly of the head of bacteriophage T4. *Nature* *227*, 680–685.

Litvinov, S.V., and Hilkens, J. (1993). The epithelial sialomucin, episialin, is sialylated during recycling. *J. Biol. Chem.* *268*, 21364–21371.

Lloyd, K.O., Burchell, J., Kudryashov, V., Yin, B.W.T., and Taylor-Papadimitriou, J. (1996). Comparison of O-linked carbohydrate

- chains in MUC-1 mucin from normal breast epithelial cell lines and breast carcinoma cell lines. *J. Biol. Chem.* *271*, 33325–33334.
- Matzuk, M.M., Krieger, M., Corless, C.L., and Boime, I. (1987). Effects of preventing O-glycosylation on the secretion of human chorionic gonadotropin in the Chinese hamster ovary cells. *Proc. Natl. Acad. Sci. USA* *84*, 6354–6358.
- Mostov, K., de Bruyn Kops, A., and Deitcher, D.L. (1986). Deletion of the cytoplasmic domain of the polymeric immunoglobulin receptor prevents basolateral localization and endocytosis. *Cell* *47*, 359–364.
- Oka, J.A., Christensen, M.D., and Weigel, P.H. (1989). Hyperosmolarity inhibits galactosyl receptor-mediated but not fluid phase endocytosis in isolated rat hepatocytes. *J. Biol. Chem.* *264*, 12016–12024.
- Oosterkamp, H.M., Scheiner, L., Stefanova, M.C., Lloyd, K.O., and Finstad, C.L. (1997). Comparison of MUC-1 mucin expression in epithelial and non-epithelial cancer cell lines and demonstration of a new short variant form (MUC-1/Z). *Int. J. Cancer*, 87–94.
- Pandey, P., Kharbanda, S., and Kufe, D. (1995). Association of the DF3/MUC1 breast cancer antigen with Grb2 and the Sos/Ras exchange protein. *Cancer Res.* *55*, 4000–4003.
- Poland, P.A., Kinlough, C.L., Rokaw, M.D., Magarian-Blander, J., Finn, O.J., and Hughey, R.P. (1997). Differential glycosylation of MUC1 in tumors and transfected epithelial and lymphoblastoid cell lines. *Glycoconjugate J.* *14*, 89–96.
- Reddy, P., Caras, I., and Krieger, M. (1999). Effects of O-linked glycosylation on the cell surface expression and stability of decay-accelerating factor, a glycopospholipid-anchored membrane protein. *J. Biol. Chem.* *264*, 17329–17336.
- Remaley, A.T., Ugorski, M., Wu, N., Litzky, L., Burger, S.R., Moore, J.S., Fukuda, M., and Spitalnik, S.L. (1991). Expression of human glycoporphin A in wild type and glycosylation-deficient Chinese hamster ovary cells. *J. Biol. Chem.* *266*, 24176–24183.
- Remaley, A.T., Wong, A.W., Schumacher, U.K., Meng, M.S., Brewer, H.B., and Hoeg, J.M. (1993). O-linked glycosylation modifies the association of apolipoprotein A-II to high density lipoproteins. *J. Biol. Chem.* *268*, 6785–6790.
- Rock, K.L., Gramm, C., Rothstein, L., Clark, K., Stein, R., Dick, L., Hwang, D., and Goldberg, A.L. (1994). Inhibitors of the proteasome block the degradation of most cell proteins and the generation of peptides presented on MHC class I molecules. *Cell* *78*, 761–771.
- Rodman, J.S., Seidman, L., and Farquhar, M.G. (1986). The membrane composition of coated pits, microvilli, endosomes, and lysosomes is distinctive in the rat kidney proximal tubule cell. *J. Cell Biol.* *102*, 77–87.
- Rosen, S.D., and Bertozzi, C.R. (1994). The selectins and their ligands. *Curr. Opin. Cell Biol.* *6*, 663–673.
- Röttger, S., White, J., Wandall, H.H., Olivo, J.-C., Stark, A., Bennett, E.P., Whitehouse, C., Berger, E.G., Clausen, H., and Nilsson, T. (1998). Localization of three human polypeptide GalNAc-transferases in HeLa cells suggests initiation of O-linked glycosylation throughout the Golgi apparatus. *J. Cell Sci.* *111*, 45–60.
- Rye, P.D., Price, M.R., Hilgers, J., and Nustad, K. (1998). ISOBM TD-4 international workshop on monoclonal antibodies against MUC1. *Tumor Biol.* *19*, 1–151.
- Scheiffele, P., Peränen, J., and Simons, K. (1995). N-glycans as apical sorting signals in epithelial cells. *Nature* *378*, 96–98.
- Schmid, S.L. (1997). Clathrin-coated vesicle formation and protein sorting: an integrated process. *Annu. Rev. Biochem.* *66*, 511–548.
- Skretting, G.D.B., van Deurs, B., Lyngaas Torgersen, M., and Sandvig, K. (1999). Endocytic mechanisms responsible for uptake of GPI-linked diphtheria toxin receptor. *J. Cell Sci.* *112*, 3899–3909.
- Trowbridge, I.S., and Helenius, A. (1998). Lectins as chaperones in glycoprotein folding. *Curr. Opin. Struct. Biol.* *8*, 587–592.
- Ulmer, J.B., and Palade, G.E. (1989). Targeting and processing of glycoporphins in murine erythroleukemia cells: use of bredelfin A as a perturbant of intracellular traffic. *Proc. Natl. Acad. Sci. USA* *86*, 6992–6996.
- Wertz, G.W., Krieger, M., and Ball, L.A. (1989). Structure and cell surface maturation of the attachment glycoprotein of human respiratory syncytial virus in a cell line deficient in O glycosylation. *J. Virol.* *63*, 4767–4776.
- Yeaman, C., Le Gall, A.H., Baldwin, A.N., Monlauzeur, L., Le Bivic, A., and Rodriguez-Boulan, E. (1997). The O-glycosylated stalk domain is required for apical sorting of neurotrophin receptors in polarized MDCK cells. *J. Cell Biol.* *139*, 929–940.
- Zanni, E.E., Kouvatzi, A., Hadzopoulou-Cladaras, M., Krieger, M., and Zannis, V.I. (1989). Expression of ApoE gene in Chinese hamster cells with a reversible defect in O-glycosylation. *J. Biol. Chem.* *264*, 9137–9140.
- Zrihan-Licht, S., Baruch, A., Elroy-Stein, O., Keydar, I., and Wreschner, D.H. (1994). Tyrosine phosphorylation of the MUC1 breast cancer membrane proteins cytokine receptor-like molecules. *FEBS Lett.* *356*, 130–136.